Experimental Investigation of Passive Enhancement of Damping for Space Structures

Nesbitt W. Hagood* and Edward F. Crawley†
Massachusetts Institute of Technology, Cambridge, Massachusetts 02139

This work presents experiments conducted to verify kinetic- and strain-energy damping enhancement schemes for large/precision space structures. Two types of damping mechanisms were applied to a 5-m-long, 10-bay aluminum cubic box truss with a quasi-free-free suspension. Tunable proof-mass dampers were implemented with space-realizable linear electromechanical drivers. Tunable piezoelectric truss members were designed and constructed for the demonstration of resonant shunted piezoelectric damping concepts. The truss damping was measured and compared with analytical predictions. The proof-mass damper implementation was found to increase the first mode damping ratio from 0.6% of critical to 6.4% of critical with a 2.7% system mass increase. The resonant shunted piezoelectric implementation increased the first mode damping ratio to 6.0%, with a 1.9% increase in system mass.

I. Introduction

DIFFICULTY arises in the control of space structures due to their densely spaced undamped modal nature. Since the actual system modes are rarely in complete agreement with the model, even the modeled modes pose some threat to the stability of the closed loop system. In addition, lightly damped modes can exist in the rolloff region of the control system. Although these modes are not included in the model, they are still subject to control authority that has not yet rolled off. These rolloff modes pose another threat of instability to the control designer.

Structural passive damping is important to the control designer as a partial solution to these two robustness issues. The need for passive damping in space structures is presented in numerous sources (see, for example, Refs. 1 and 2). Damping tends to displace the structural poles toward the left in the typical s-plane representation. This extra room gives the passively damped system more robustness to modeling error in the control system and helps alleviate the problems associated with structural modes in the rolloff region of the controller.

There are several sources of passive damping on space structures. The most common is material damping by which structural strain energy is dissipated. Damping is also provided by the friction and impacting that occur in the structural joints. The inherent damping in a truss can be increased by using damping enhancement schemes (Ref. 3). Several damping techniques are applicable to space structures. Some viscoelastic techniques have been developed for trusses in Ref. 4. Proof-mass dampers (PMDs) have been applied previously to space structure damping in Ref. 5 and conceptually in Ref. 6. Truss structures with active piezoelectric members for vibration suppression are presented in Refs. 7 and 8. This work will present implementations of both classical tuned vibration absorbers and a new passive damping application using piezoelectric members.

The objective of this work is to investigate two methods of damping enhancement for a lightly damped truss structure. These damping schemes are the classical PMD and the resonant shunted piezoelectric (RSP). These concepts will be implemented on a realistic structure to provide experimental verification of these damping enhancement mechanisms. In addition, the utility of a frequency-domain systems analysis for modeling damped structures presented in Ref. 9 will be examined.

Section II outlines the main design challenges of the experiment: the design of the test bed for the damping experiments and the implementation of the damping devices under investigation, linear proof-mass damper/actuators (PMD/A) and piezoelectric truss members. Section III presents the results of the experimental investigation. The experimental results for the dynamics of a truss structure with the described damping mechanisms are presented and compared with the analytical results obtained from frequency-domain modeling. The sensitivities of the system damping levels to variation of the resonant dampers' tuning parameters are also presented.

II. Experimental Setup and Design

In this section, the experimental program will be discussed along with the attendant hardware development. This hardware falls into three categories: underlying structure to be tested, actuators/dampers used to implement the damping schemes, and electronics necessary to support these dampers and gather data for the investigation.

Truss Structure and Setup

A truss was designed and constructed for use as a test bed for the damping enhancement schemes. The truss had to meet several requirements. First, the truss had to exhibit low inherent damping levels. This was necessary so that the increase in damping due to the proposed damping schemes could be measured easily. Second, it was desirable to have a simple, understandable yet realistic test structure so that physical insight could be used to readily interpret the results.

The truss structure presented in Fig. 1 was constructed to meet these requirements. The truss was constructed from commercial hardware from MERO-Raumstruktur GMBH & Company. The total experimental truss length was 5 m, consisting of 10 cubic bays of 0.5 m. The bay geometry and internal diagonal positioning are shown in Fig. 1. The elements of the truss consisted of steel nodes and aluminum tubular members for the battens, diagonals, and longerons. The steel nodes each massed 0.228 kg. The longerons and battens massed 0.202 kg, with a modulus of 68.8 GPa, a cross-sectional area of 6.31×10^{-5} m^2, an effective length of 0.398 m, and an ex-

Presented as Paper 89-3436 at the AIAA Guidance, Navigation, and Control Conference, Boston, MA, Aug. 14–16, 1989; received Dec. 15, 1989; revision received July 2, 1990; accepted for publication July 9, 1990.

*Assistant Professor, Department of Aeronautics and Astronautics, Rm. 33-313. Member AIAA.

†Professor, Department of Aeronautics and Astronautics, Rm. 37-341. Member AIAA.

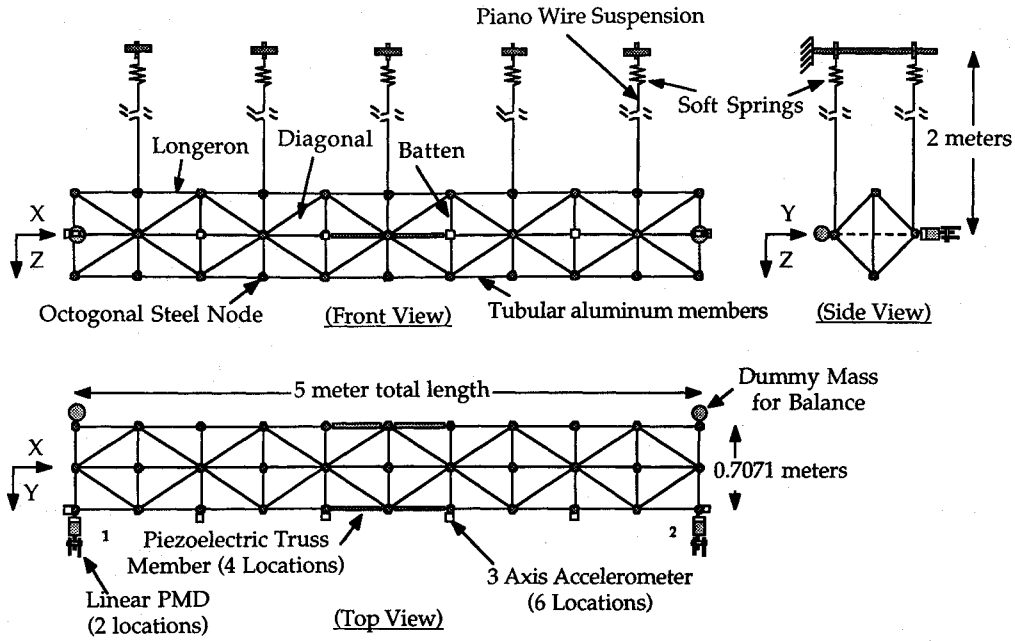

Fig. 1 Truss geometry, and actuator and sensor placement. The structure was driven by the PMA at node 1 and damped by either the PMD at node 2 or by the four piezoelectric truss members.

ternal diameter of 22 mm. The diagonals massed 0.239 kg, with the same modulus, cross-sectional area, and external diameter as the battens but with an effective length of 0.604 m. The members bolted into the threaded nodes to create a tight, no-slop joint even under high excitation. The complete specifications of the test article can be found in Refs. 3 and 10.

Since data were desired on damping enhancement of a realistic three-dimensional space structure, unconstrained truss vibration was valuable to simulate the isolated environment of space. Isolation from the external environment was necessary to prevent energy dissipation through the boundaries. To achieve these conditions, the truss was suspended at 10 locations by 0.25-mm-diam piano wire. These wires were 2 m long, giving truss horizontal pendulum modes under 0.35 Hz. The wires were connected to soft coil-steel springs to give a 1.2-Hz vertical bounce mode. The support wires are adjustable to distribute evenly the truss weight among themselves, helping to eliminate support deformations and stresses. The frequency separation between the truss modes (first bending at 39 Hz) and the low bounce (1.2 Hz) and pendulum support modes (0.35 Hz) helped to isolate dynamically the truss from external interaction and also allowed the truss to exhibit essentially free-free behavior in the first three X-Y bending modes.

The truss was outfitted with 18 PCB Model 330A accelerometers for structural response sensing and mode shape imaging. The accelerometers were organized into six 3-axis sets located on the truss, as shown in Fig. 1. In all of the structural dynamic testing, the truss was excited using the proof-mass actuator (PMA) at node 1. For the PMD experiments, a PMD replaced a dummy mass at node 2. For the shunted piezoelectric experiments, four standard aluminum members in the central two bays of the truss were replaced by piezoelectric members in the X-Y plane as shown in Fig. 1.

Proof-Mass-Damper Implementation

The first damping methodology tested was the classical PMD or tuned mechanical vibration absorber (Ref. 11). It involved a mass connected to a structure via a spring and a dashpot. The parameters of the spring and dashpot can, in principle, be tuned for maximum energy dissipation. The objective of the present PMD design was to produce an easily tunable, mass efficient mechanical vibration absorber for damping augmentation.

The PMD design is presented in Fig. 2. The heart of the PMD was a permanent field, linear drive dc motor consisting of two main elements: a permanent magnet and surrounding magnetic material for the production of a uniform magnetic field; and a drive coil through which current passes to produce a reaction force against the magnetic field. This is the same principle of operation as a conventional acoustic speaker or dynamic shaker. In the linear PMD implementation of Fig. 2, the drive coil was attached to the structure, and the heavy magnet and magnetic material necessary to produce a radial field served as the proof mass. The permanent magnet was a ring with 5.08-cm outer diameter, 2.54-cm inner diameter, and axial thickness of 1.27 cm.

The magnetic mass was supported by a stainless steel axial rod. The entire damper (except for the displacement and velocity transducers) was axially symmetric about this rod. The proof mass was free to move along the axial rod on a set of precision linear bearings manufactured by Thompson Linear Bearings. This overall damper design is similar to the one used for the NASA/University of Virginia (UVA) inertial actuator (Ref. 12).

The proof mass was centered on the rod by two steel springs. The springs provided the base stiffness for the PMD, creating a system with resonance at 11 Hz. The remaining stiffness and viscous damping necessary to tune the PMD to the structural modes from 11 to 120 Hz were provided electrically via position and velocity feedback. The position was measured by a Trans-tek linear variable displacement transducer (LVDT) mounted as shown in Fig. 1. The velocity was measured by a Trans-tek linear velocity transducer (LVT) mounted alongside the LVDT. The feedback gains could be varied easily to tune the PMD to a structural mode.

The total mass of the proof mass was minimized by using high permeability magnetic materials for the conduction path and high-energy-density neodymium-iron-boron permanent magnets. A comparison of mass ratios for a similar linear actuator, the NASA/UVA linear PMA (Ref. 11), highlights the mass efficiency of the present design. The mass efficiency of a PMA can be measured as the ratio of total mass to proof mass. This proof-mass ratio for the present design is 0.74 compared with 0.33 for the NASA/UVA PMA. The present

design has a total mass of 1.87 kg. The ratio of maximum force to total weight can also be interpreted as a measure of mass efficiency. The ratio is 1.21 for the present design compared with 0.62 for the NASA/UVA PMA.

Four PMDs were calibrated both statically and dynamically. In the static tests, the proof mass was held fixed relative to a rigid base, and the force generated for a given input current was measured. The present design had an average force-to-current ratio of 4.45 N/A. In the dynamic tests, the resonant frequencies and damping of the PMDs were measured with the PMDs attached to a rigid base and the proof mass free. Ring-down tests were conducted on the resonator both for the open-loop plant and with position and velocity feedback. The open-loop plants were found to have a resonance at 11.2 Hz due to the positioning springs and friction damping force of 0.45 N. The PMD could be tuned in the range of from 11 to 120 Hz with a viscous damping ratio of from 1 to 45% of critical by varying position and velocity feedback gains. The device could be used both as a classical proof mass damper with appropriate tuning or as a linear inertial actuator. The PMD/As built were used both as a driver at node 1 and as a damper at node 2 in the experiments on the truss.

Piezoelectric Truss Member Design

The design and manufacture of the piezoelectric truss members used to implement the resonant shunted piezoelectric (RSP) damping enhancement concept will be presented in this section. The goal of the design was to produce lightweight, variable length truss members that could be used either as part of an active control scheme for the truss or as passive dampers (as presented in this work). The use of piezoelectric materials as resonant dampers after the addition of appropriate circuitry has been presented previously in Ref. 13. The implementation of this concept entailed the construction of piezoelectric truss members to replace the standard aluminum truss members.

Four piezoelectric longeron truss members were manufactured to replace four members in the center two bays of the truss, as shown in Fig. 1. The members were placed so as to maximize the precentage of modal strain energy in the piezoceramics for the first and third X-Y bending modes. The piezoelectric members are wired together so that a single voltage across the combined electrode causes the two members on one side to contract while the two members on the other side expand. In this way, the combined piezoelectric members are well coupled to bending modes that have high strain in the central bays.

The design of the piezoelectric member consisted of three main elements. The first was a hollow piezoceramic tube extending the length of the member. The second element in the design was the fittings that attached to the ceramic stack and allowed the member to be connected to the truss in the same fashion as the aluminum members. The third element was the composite shell built up around the piezoceramic stack to provide continuity and strength to the member. These elements

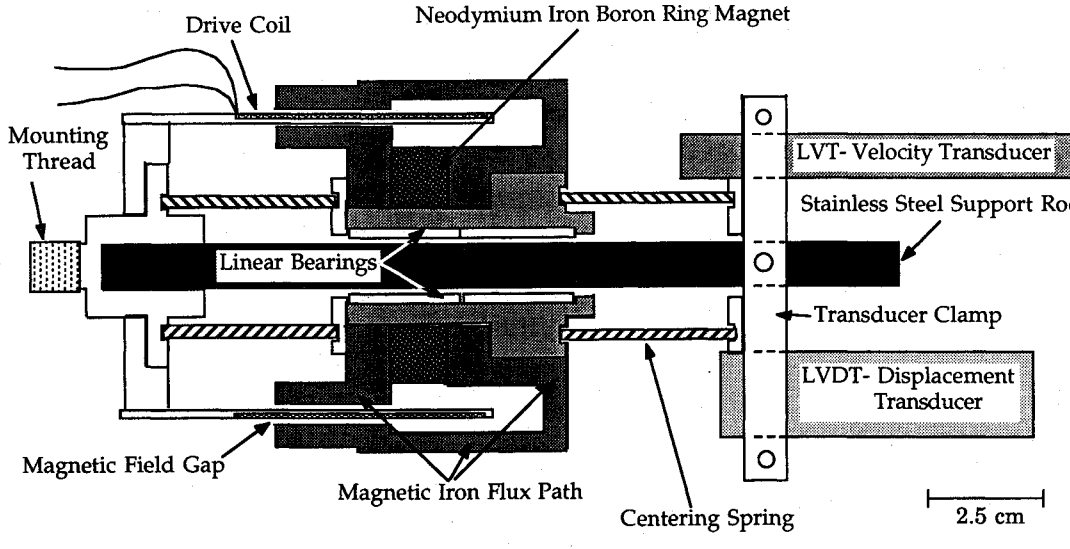

Fig. 2 PMD schematic showing drive coil, proof mass, and sensors.

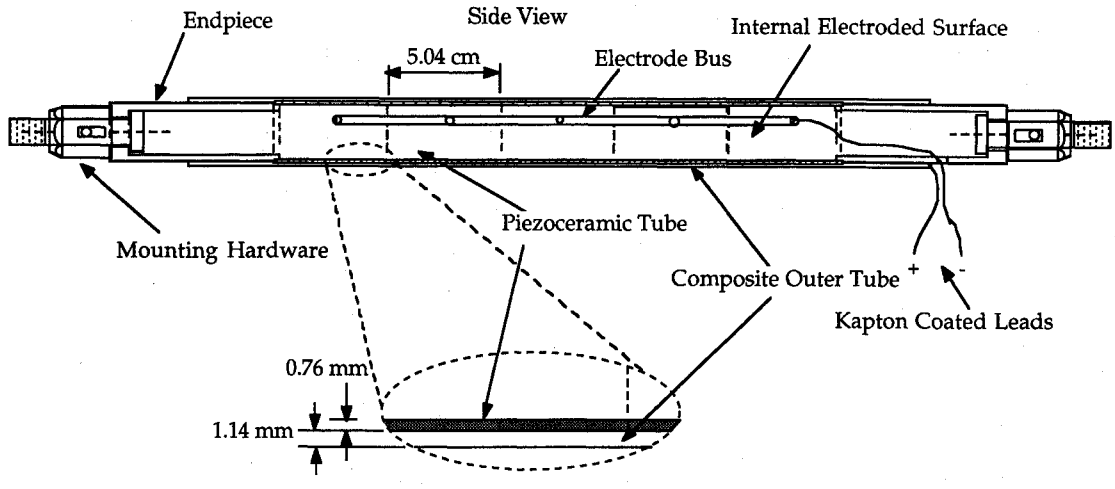

Fig. 3 Piezoelectric truss member schematic showing positioning of piezoceramic tubes, composite shell, and endpieces.

are shown in the layout of the piezoelectric truss member shown in Fig. 3.

The operative component of the member was the piezoelectric stack. The stack consists of five piezoceramic tubes bonded together. The piezoceramic tubes were made with PZT-5H material from Vernitron Piezoelectric Company (Ref. 14). The individual piezoelectric tubes were 5.04 cm long, with an outer diameter of 2.54 cm, and a wall thickness of 0.76 mm. The cylinders had electrodes on their interior and exterior surfaces and were poled in the radial direction. Thus, when a voltage was applied across the electrodes, the piezoelectric expanded axially in proportion to the d_{31} piezoelectric constant defined in Ref. 14. Five tubular elements were bonded endwise to create a total piezoceramic stack 25.20 cm long.

The internal and external electrodes were each electrically connected to common internal and external electrical buses. This enabled the entire stack to behave as one large piezoelectric tube electroded on its inside and outside surfaces. This piezoceramic stack was fitted with aluminum endpieces, which allow the truss member to be inserted in the truss by bolting to the nodes. The stack and endpieces were wrapped with a composite shell, which coats the piezoceramics and edges of the endpieces. Glass-epoxy composite material was used for ease of manufacture and to prevent shorting between the truss and the external piezoceramic electrode.

The composite shell serves primarily to increase the strength of the member but not the stiffness. The piezoceramic material is very stiff (Young's modulus of 60.6 GPa) by nature and very brittle. The addition of the composite tends to increase the fracture toughness of the member and thus make it useful as a structural member. The stiffness of the member is still primarily due to the piezoceramic (80% of the stiffness) since the composite tends to act only as a shear layer to convey stress across the defects and bonds in the piezoceramic stack.

The total mass of the piezoelectric members was 0.320 kg. The total stiffness of the members was 1.94×10^7 N/m, which was slightly stiffer than the standard aluminum members. This stiffness was calculated from the change in first truss frequency when the piezoelectric members were inserted into the truss. The static force capability of the members was calibrated by measuring the force generated by the member as it expanded against fixed end constraints. The average for the members was 634 N at a maximum voltage of $\pm$ 450 V before the piezoelectric material depoled. In free expansion, this voltage corresponded to a stroke of $\pm$ 32.5 μm.

Damper effectiveness is increased by concentrating most of the member strain energy in the piezoelectric material. The loss factor that can be achieved with the member is the sum of the loss factors for the ceramic and the composite weighted by the proportion of strain energy in each. The loss factor of the piezoelectric is increased by shunting an electrical impedance across the electrodes of the ceramic stack. This shunting, and the electrical support that enables it, is described in the following section.

Table 1 Experimental and analytical modal natural frequencies and damping ratios for truss with PMD at node 2

	Baseline aluminum		PMD tuned to mode 1		PMD tuned to mode 2	
Mode	Exp.	Anal.	Exp.	Anal.	Exp.	Anal.
	Natural frequencies, Hz[a]					
1a	39.2	39.2	35.7	36.5	38.6	39.1
1b	—	—	43.4	43.0	—	—
2a	99.4	91.1	99.9	92.4	95.0	89.2
2b	—	—	—	—	106.6	—[c]
3	149.0	146.6	151.5	147.4	150.8	147.4
	Damping ratios, ζ[b]					
1a	0.0063	0.0061	0.0619	0.0727	0.0090	0.0066
1b	—	—	0.0642	0.0885	—	—
2a	0.0048	0.0040	0.0065	0.0063	0.0413	0.0210
2b	—	—	—	—	0.0562	—[c]
3	0.0030	0.0036	0.0101	0.0035	0.0085	0.0035

[a]Natural frequency accuracies are $\pm$0.5% for $\zeta<2\%$ and $\pm$5% for $\zeta>2\%$.
[b]Damping ratio accuracies are $\pm$5% for $\zeta<2\%$ and $\pm$20% for $\zeta>2\%$.
[c]Analytical model does not exhibit mode splitting due to resonant damper.

Piezoelectric Member Support Electronics

Piezoelectric materials typically have been used as active elements in structural vibration control systems where they produce a strain for a commanded voltage (Refs. 15-18). They can also be used to augment structural passive damping by shunting an appropriate passive impedance across the piezoelectric electrodes. The electrical shunting impedance couples with the inherent capacitance of the piezoelectric material to modify the piezoelectric materials' stiffness and damping properties in a predictable fashion. By appropriate choice of the shunting impedance, the structural passive damping can be maximized for a given mode or group of modes (Ref. 13).

If a resistor is used to shunt the piezoelectric electrodes, the piezoelectric material behaves as if it were a first-order viscoelastic material. The resistor dissipates the electrical energy that has been converted from mechanical energy by the piezoelectric material and, thus, increases the material loss factor. If a resistor and inductor in series are shunted across the piezoelectric electrode, then a resonant electrical circuit is created with the inherent piezoelectric capacitance. The parameters of the resonant electrical circuit, its frequency and damping, can be chosen to increase greatly the damping in a given structural mode. The electrical resonance is coupled to

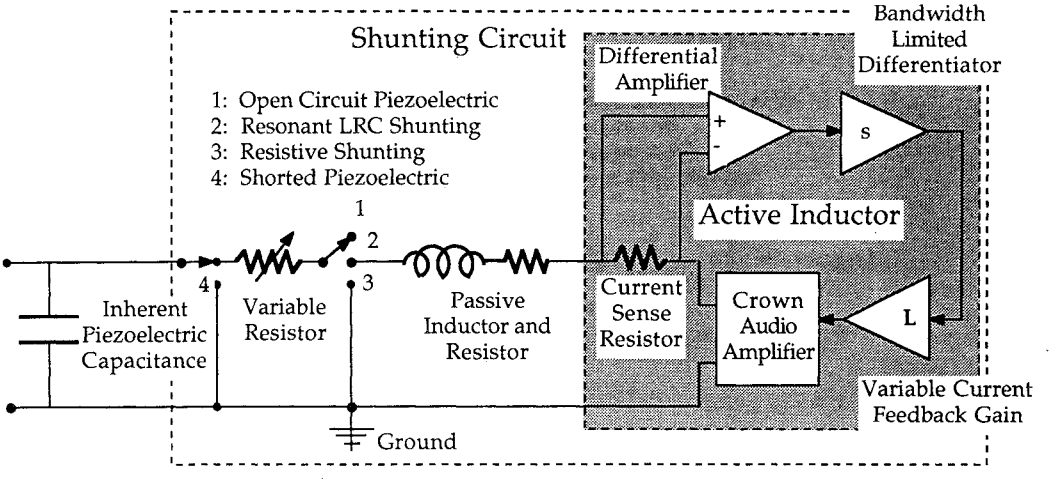

Fig. 4 Shunted piezoelectric support circuitry showing passive and "active" inductors as well as variable resistance.

the mechanical resonance through the piezoelectric. This RSP is the electrical analogy to a resonant mechanical vibration absorber or PMD and can be tuned likewise to a structural mode to maximize damping.

A shunting circuit was designed that enabled the combined piezoelectric damper (four members wired together) to be either resistively shunted, resonantly shunted, or shorted. In the resistive case, the shunting circuit has a variable resistor. In the resonant case, this circuitry contains a variable resistor and a fixed and variable inductor in series. The variable inductor is necessary for tuning the electrical resonant frequency to the vicinity of the truss modes.

The overall shunting circuit architecture is shown in Fig. 4. It is attached to the electrode of the combined piezoelectric damper. The circuit allowed the damper to be left open, shorted, shunted with a resistor, or shunted with a resistor-inductor circuit, depending on the position of the switches. The piezoelectrics were driven by a Crown 300-IIA voltage amplifier with voltages up to ± 45 V (far below maximum).

For a small piezoelectric capacitance and low structural modes, the optimum tuning results for the RSP (Ref. 13) require large inductance while maintaining low electrical resistance. The low combined piezoelectric capacitance (2.17 μF) necessitated the use of large inductances for tuning the piezoelectric to the lower structural modes. To tune to the first structural mode at 39 Hz, a 7.0-H inductance and 230-Ω resistance were required. Such large inductance is normally associated with a large series resistance. To circumvent this problem, low-resistance passive inductors were used in series with an active variable inductor. The 7.0-H passive inductor massed only 268 g and, thus, was only a small fraction (0.5%) of the total system mass.

The active variable inductor used for tuning the electrical resonance was constructed using current rate feedback, as shown in Fig. 4. An active inductor was needed only to facilitate tuning for the experiment and could have been replaced by a passive component. The Crown amplifier commanded a voltage across its output that was proportional to the rate of current going through the output stage of the amplifier. The circuit reproduced the defining relation for an inductor. By varying the gain on the feedback current rate, the inductance for this circuit could be varied. This enabled the resonant electrical circuit to be tuned to the structural modes.

III. Damping Enhancement Tests

Two types of resonant damping devices were implemented on the truss for damping enhancement. The two devices considered were PMDs and RSP truss members. Both devices could be tuned simply to a structural mode, as described in the previous sections.

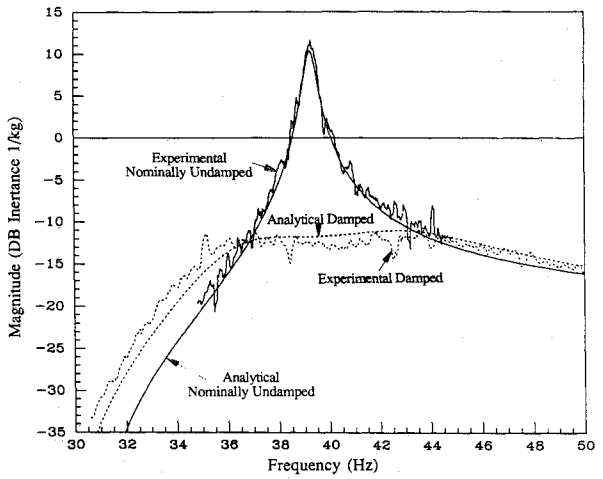

Fig. 5 Results for nominally undamped and PMD damped truss: comparison of experimental and analytical transfer functions from node 1 forcing to *Y*-direction acceleration.

Two types of tests were conducted with these damping mechanisms. The first involved optimally tuning the damper to the structural mode of interest and identifying the resultant modal frequencies and damping of the truss. The second type of test entailed varying the resonant parameters of the devices in the vicinity of the optimal tuning conditions and recording the resulting variation of the global system frequencies and damping. This type of test provides sensitivity information useful in damping enhancement system design and verification.

In all of the tests, the modal frequencies and damping for the first, second, and third X-Y bending modes of the truss were identified with a recursive lattice least-squares (RLLS) algorithm (Ref. 19). The identification was performed on the time-averaged response of the truss to a white noise force input by the PMA at node 1. The response was measured by the accelerometer at node 1 in the Y direction. The RLLS algorithm satisfactorily identified the modal frequencies and damping of the lightly damped modes ($\zeta < 2\%$) to an accuracy of about $\pm 0.5\%$ on the frequencies and $\pm 5\%$ on the damping ratios, repectively. For highly damped ($\zeta > 5\%$), closely spaced modes, the RLLS algorithm was very imprecise, varying as much as 5% on the frequencies and $\pm 20\%$ on the damping ratios identified.

Tests with Nominally Undamped Aluminum Truss

The first stage of testing involved the identification of the lightly damped all-aluminum truss with a dummy mass in place of the PMD at node 2 in Fig. 1. These data were used for comparison of the damping increase afforded by the PMD. As shown in Table 1, the nominal truss had bending modes at 39.2, 99.4, and 149.0 Hz with 0.63, 0.48, and 0.30% damping, respectively.

An analytical model was developed for the truss based on the frequency-domain analysis presented in Ref. 9. The truss elements are modeled by their frequency dependent mechanical impedances and assembled to form a global impedance model of the truss. The location of the system eigenvalues can be found by locating the zeros of the determinant of the global impedance matrix. Locating the zeros involves a numerical search over the complex plane. The results for the poles of the nominal system are shown compared with the experimental poles in Table 1. The parameters of the model were adjusted once so that the frequency and damping of the first mode of the all-aluminum nominal truss model agreed with the identified experimental values. This led to close model agreement to the third bending mode but a relativly large error in the second bending mode natural frequency. The error in the second mode natural frequency may be attributed to incorrect modeling of the stiffness of the diagonal members relative to the longerons.

Tests with Optimally Tuned Proof-Mass Dampers

For the optimally tuned PMD tests, the damper described previously was placed at node 2, as shown in Fig. 1 (replacing the dummy mass used in the nominal truss tests). The electrical state-feedback scheme enabled the device to be tuned alternately to the first two horizontal bending modes of the truss.

The first test in this series was to tune the damper to the first bending mode of the all-aluminum truss at 39 Hz. Based on the analytical model, the ratio of damper mass to system modal mass (not total mass), called β in PMD terminology, was found to be 3% for the first mode. The frequency to which the PMD is tuned as well as the damping ratio of the PMDs mechanical resonance are determined by this mass ratio. In PMD terminology, the frequency tuning of the damper is specified by the parameter δ, which is defined as the ratio of damper resonant frequency over the structure natural frequency (ω_d/ω_n). The damping of the PMD resonance is specified by the parameter r, which is defined as twice the vis-

cous damping ratio of the PMD (2ζ). For the analytically determined β of 3%, the optimal value of the tuning parameter δ_{opt} is 0.97, and the optimal value of the dissipation parameter r_{opt} is 0.25 (Ref. 11). These values were used as a first guess for the PMD tuning.

The actual optimal tuning of the damper to the test structure was found by visual inspection of the experimental transfer function. The transfer function from forcing at node 1 to acceleration in the y direction at node 1 was recorded and displayed by a Textronix 2630 Fourier analyzer. The peak value of the displayed transfer function was minimized by comparing successive transfer functions while varying the feedback gains. The experimentally determined optimal frequency tuning parameter $\delta_{opt\text{-}exp}$ was 0.955, and the experimentally determined optimal dissipation parameter $r_{opt\text{-}exp}$ was 0.296. These values agree closely with the analytical guesses. The experimental frequency tuning was slightly lower than the analytical value, which indicates that the modal mass fraction was slightly larger in the experiment than in the model.

The results from the damping enhancement tests with the PMD tuned to the first mode are shown in Table 1 with comparisons to the analysis and the all-aluminum truss dynamic tests. As expected, the PMD replaces the structural mode to which it is tuned with two highly damped modes. The PMD gives damping levels as high as 6.4%. It provides this damping only to the mode to which it is tuned. There is almost no "spillover" of damping into the second mode. The third mode damping is the result of damper rattle at that high frequency and cannot be attributed to PMD residual damping.

The experimental results can be seen compared with the analytically derived pole locations in Table 1. There are two model modes at first bending due to the PMD, but these modes are more highly damped than the experimental modes identified by the RLLS algorithm. The exact model frequencies for the first mode are within 2.1% of the experimental frequencies. The frequencies calculated for the higher modes reflect the errors present in the initial modeling of the nominal truss. The damping predicted from the analytical pole locations is higher than the experimental damping but correctly predicts the large increase in first mode damping due to the PMD. The error between the experimentally determined and analytically derived first mode damping estimates could be manifestations of the RLLS identification algorithm, as explained previously.

Another point of interest is the "fallout" damping afforded to the second bending mode by the damper tuned to the first mode. The experimental second mode damping rose from 0.48% critical in the all-aluminum truss to 0.65% in the PMD damped truss in the second mode. The model correctly predicts this increase in the second mode damping as shown in Table 1. The model damping rises from 0.40% of critical to 0.63%, representing a 2.6% error from the experimental for the damping in the second mode of the PMD damped truss.

The system transfer function for the first mode from the forcing point to the Y direction acceleration at node 1 can be seen compared with the equivalent all-aluminum truss transfer function and the analytical model results in Fig. 5. The PMD decreases the amplitude of structural response in the first mode by over 22 dB with a total system mass increase of 2.7%.

The analytical transfer function for the damped and undamped first mode compares very well with the test results. The close correlation between the experimental and theoretical transfer functions implies that the frequency-domain modeling technique presented in Ref. 9 accurately models the PMD damped structure.

The PMD at node 2 was also tuned to the second structural mode via the feedback circuitry described previously. The optimal damper parameters were found as before by visual inspection of the experimental transfer function to be $\delta = 0.977$ and $r = 0.272$. These agree well with the analytically derived optimal tuning parameter, $\delta = 0.977$, and damping parameter, $r = 0.306$.

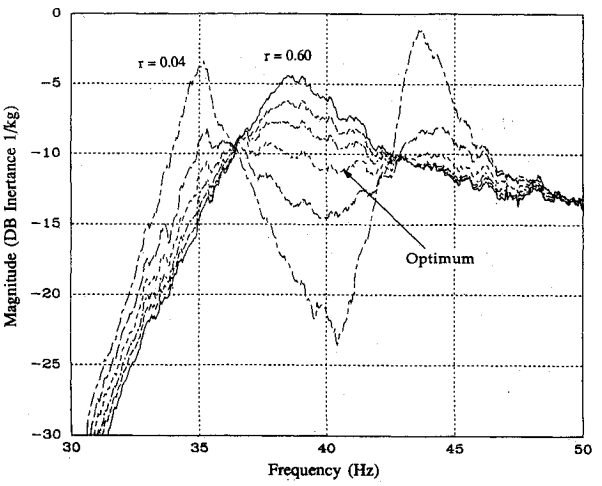

Fig. 6a First mode PMD dissipation parameter variation from $r = 0.04$ (widely spaced modes) to $r = 0.60$ (single mode).

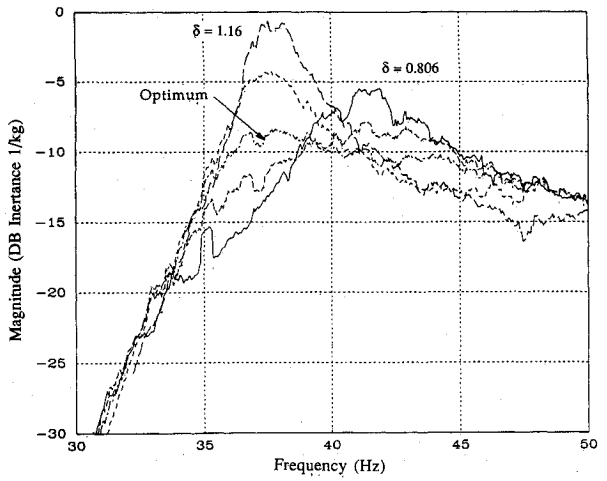

Fig. 6b First mode PMD frequency tuning parameter variation from $\delta = 0.806$ (single mode above 40 Hz) to $\delta = 1.16$ (single mode below 40 Hz).

The results for the dynamic characteristics of the truss test modes for second mode tuning are presented compared with the analytical model and the nominal truss results in Table 1. From these data, the effectiveness of the PMD in damping the second mode is evident. The damper tuned to the second mode increased the second mode damping from 0.48% of critical in the all-aluminum truss experiments to 4.1 and 5.6% for the upper and lower branches of the second mode of the PMD damped truss, respectively. The damper has little effect on the first and third modes of the truss.

The model fails to reflect the splitting of the second truss bending mode due to the tuning of the PMD. Although the PMD is optimally tuned to the experimental second bending mode, it is not optimally tuned to the model second mode because the model mode has a natural frequency different from the experimental mode, as explained previously. As a result, the PMD is tuned far above the second model mode and does not influence the global structural dynamics other than to increase the second mode damping by a small amount.

These tests on the effectiveness of PMDs at optimal tuning yield some interesting insights into the practical aspects of damping enhancement for space structures. First, the PMDs are mass-efficient, contributing an average of 6.3% critical damping for a total system mass ratio of about 2.7% with little variation of the base structure's modes. This mass did not include amplifier and feedback circuitry masses. Second, it is difficult to tune the resonant dampers accurately to the truss

Table 2 Experimental and analytical modal natural frequencies and damping ratios for truss with RSP dampers

	Baseline aluminum		RSP tuned to mode 1		RSP tuned to mode 3	
Mode	Exp.	Anal.	Exp.	Anal.	Exp.	Anal.
			Natural frequencies, Hz[a]			
1a	39.4	40.0	38.3	38.8	39.5	39.9
1b	—	—	43.7	44.6	—	—
2	99.0	91.5	99.3	92.2	99.2	91.0
3a	145.5	145.0	145.2	146.0	144.4	139.5
3b	152.8	—[c]	152.0	—[c]	152.0	150.5
			Damping ratios, ζ[b]			
1a	0.0119	0.0117	0.0418	0.0248	0.0108	0.0121
1b	—	—	0.0599	0.0566	—	—
2	0.0062	0.0056	0.0056	0.0054	0.0057	0.0062
3a	0.0095	0.0044	0.0113	0.0044	0.0132	0.0207
3b	0.0115	—[c]	0.0100	—[c]	0.0121	0.0155

[a]Natural frequency accuracies are ±0.5% for $\zeta<2\%$ and ±5% for $\zeta>2\%$.
[b]Damping ratio accuracies are ±5% for $\zeta<2\%$ and ±20% for $\zeta>2\%$.
[c]Analytical model does not exhibit mode splitting due to resonant damper.

using the analytical model alone since small variations in the model produce large variations in the damping levels realized on the truss. This necessitates some sort of variable tuning scheme in the actual implementation to achieve the theoretical damper performance.

Frequency and Damping Sensitivities to Proof-Mass-Damper Parameter Variation

Tests were conducted on the truss structure with the PMD parameters tuned in the vicinity of, but not at optimum tuning for, the first truss bending mode. Once the optimal tuning parameters had been determined in the previous test, the tuning parameters of the PMD were varied in a pattern about this optimum. The purpose of the test was to determine the effect that mistuning has on the damping afforded by the resonant device. Since tuning is required with resonant devices, and the structural parameters can vary from the model used in analysis, it is useful to determine the sensitivity of the truss damping levels to mistuning.

These tests were conducted using the techniques described for the optimum tuning experiments. The feedback tuning circuit was used for the parameter variation. This test was conducted only for parameter variation about the first mode. In one variation series, the damper was set to the optimum frequency tuning δ and the damper's internal dissipation r was varied from underdamped to overdamped. In the other series, the damper was set to the optimum internal dissipation and the frequency tuning was varied from below to above optimal.

The series of transfer functions associated with the first series of damper dissipation parameter r variations is presented in Fig. 6a, and the second series with frequency tuning variation is shown in Fig. 6b. Several trends are apparent. At optimal frequency tuning, the transfer function changes with increasing dissipation parameter r from two undamped modes through optimal r to a single undamped mode as the damper internal dissipation rises.

Some interesting trends are also visible in the frequency tuning variation tests at optimal damper internal dissipation levels. As the tuning goes from below optimal to above optimal, the system transfer function lowers on the right to the optimal value, then rises on the left. The primarily structural mode moves out from the imaginary axis and becomes more highly damped as the PMD mode becomes less damped and eventually replaces it. As seen in the transfer functions, a small variation in the tuning parameters can result in a large increase of system response for PMDs.

Tests with Optimally Tuned Resonant Shunted Piezoelectrics

The piezoelectric truss members described previously were used as elements of a resonant damping enhancement scheme for space structures. Four members in the central bays of the all-aluminum truss in the configuration in Fig. 1 were replaced by four piezoelectric truss members. The truss was otherwise undamped and driven by a PMD driver at node 1. The truss members on opposite sides of the truss were wired with opposite polarity so as to cause the members on one side to expand as the others contracted. The four piezoelectric members thus were wired to create one combined piezoelectric damper that was sensitive to bending. This total damper was used to test the performance of the RSP damping concept.

The first step in the testing was to establish the modal parameters of the nominal undamped truss. To isolate the effects of the shunting circuit, data were taken first with the piezoelectric members electrically shorted. The first four truss bending modes were found to be at 39.4, 99.0, 145.5, and 152.8 Hz. The damping for these modes was 1.19, 0.62, 0.95, and 1.15% of critical, respectively. The third and fourth modes are actually both third bending modes. Replacing the aluminum members with piezoelectric members caused the third X-Y and X-Z bending modes to couple, so that both were now observable from the X-Y plane.

Experiments were conducted to determine the natural frequencies and damping ratios of the truss when the piezoelectric damper had been tuned optimally to the truss structure's first or third bending mode. Tests were not performed on the second structural mode since in this mode there is little bending strain energy in the central two bays of the structure. The tuning was done in accordance with the guidelines given in Ref. 13. The natural frequency of the electrical resonance is matched approximately to the structural mode, and the damping in the electrical resonance is chosen so as to minimize the modal response.

The first resonant piezoelectric experiment entailed tuning the damper to the first structural bending mode of the nominal shorted-piezoelectric structure at 40 Hz. Whereas the PMD tuning depended on the modal mass ratio (kinetic energy ratio) β, the RSP tuning depends on the ratio of electrical energy in the piezoelectric capacitor to the structural modal strain energy. This ratio is called the generalized electromechanical coupling coefficient K_{31}^2 in Ref. 13. Based on the analytical model, this ratio was found to be 1.5% for the first mode. The frequency to which the RSP is tuned as well as the damping ratio of the RSP's electrical resonance are determined by this energy ratio. In RSP terminology, the frequency tuning of the damper is specified by the parameter δ, which is defined as the ratio of damper electrical resonant frequency over the structure natural frequency (ω_e/ω_n). The damping of the RSP resonance is specified by the parameter r, which is defined as twice the viscous damping ratio of the RSP (2ζ). For the analytically determined K_{31}^2 of 1.5%, the optimal value of the tuning parameter δ_{opt} is 1.007 (Ref. 13). The optimal value of the

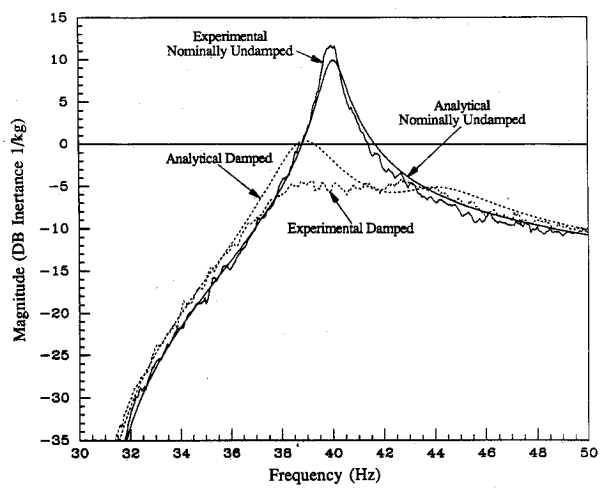

Fig. 7 Results for the nominally undamped and RSP damped truss: Comparison of experimental and analytical transfer functions from node 1 forcing to Y-direction acceleration.

dissipation parameter r_{opt} is 0.17. These values were used as a first guess for the RSP tuning.

The electrical tuning that was found to give the lowest amplitude of structural response was at an inductance of 7.29 H and resistance of 248.7 Ω along with the inherent capacitance of the four piezoelectric members of 2.17 μF. The resulting optimal frequency tuning parameter $\delta_{opt\text{-}exp}$ was 1.015, whereas the optimal dissipation parameter $r_{opt\text{-}exp}$ was 0.1336. These parameters correspond to the optimum tuning conditions for a system with a generalized coupling coefficient K^2_{31} of 3.0%. The experimental results thus exhibit a larger coupling coefficient and, therefore, more damping capability than would be expected from the analytical model.

The results for the truss structure frequency and damping ratios can be seen compared with the other piezoelectric tests and to the analytical model in Table 2. The first mode damping was increased from 1.1% critical in the shorted case to an average of 5.1% with RSP damping. This damping increase is only apparent in the first mode, just as in the PMD experiment.

In the experiments, the piezoelectrics are tuned optimally to minimize the amplitude of the system transfer function. The experimentally determined tuning parameters were then used in the analytical model. Since the analytical model frequencies do not match the experimental truss frequencies exactly, the tuning parameters that produce optimal results on the experimental truss will not necessarily produce optimal results in the model. This accounts for the discrepancies between the actual and the model first mode frequencies and damping. There was little damping spillover to the second and third truss bending modes in either the model or the experiment.

The system transfer functions of the first mode can be seen for the shorted and resonant shunted piezoelectrics compared with the analytical results in Fig. 7. The 15-dB reduction in system response indicates that the optimally tuned piezoelectric damper can be used as a modal damper with performances comparable to a PMD's. This decrease in modal amplitude was accomplished with a 1.9% increase in system total mass (including shunting circuitry). Although there is good agreement between the experimental and analytical undamped truss transfer functions, the damped transfer functions differed greatly. Mismodeling leads to inaccurate tuning in the model as opposed to the optimal tuning demonstrated by the experimental transfer function. In all, the RSPs were clearly effective as modal dampers. More work needs to be done on modeling the structural aspects of the piezoelectric truss members.

Experiments were also conducted with the piezoelectric truss members tuned to the third bending mode of the truss. All arrangements were as before for the first mode tuning. The optimum tuning conditions were found to occur with the inductance at 0.51 H, the resistance at 19.5 Ω, and the capacitance as before.

The third mode experimental results are compared with the other piezoelectric cases and with the analytical model in Table 2. Although the duality of the third mode makes it difficult for the analytical model to track the damping, a few points are clear. The shunted piezoelectric does increase the damping in the experimental truss in the third modes by about 0.4% of critical for the lower mode and about 0.1% for the upper. This is probably because the piezoelectric is coupled more strongly to the lower mode. The prediction of third mode damping suffers from inaccurate modeling of the mode to which the RSP was to be tuned. The model does predict an increase in the damping of the third mode from 0.4% in the nominal shorted piezoelectric test to 2.1% for the RSP tuned to the third mode. Thus, although the double mode typical of resonant dampers does not appear, the mistuned damper does afford an increase in damping.

The low damping authority of the experimental RSPs in the third mode can be explained by two factors. First, the strain energy in the third mode is not as concentrated into the central two bays as it is in the first mode. Second, in the experimental truss, the horizontal bending modes in the *X-Z* and *X-Y* planes coupled to produce two modes that were not as observable/controllable from the piezoelectrics as a pure horizontal mode would have been.

Sensitivities to Resonant Shunted Piezoelectric Parameter Variations

Tests were conducted with the RSP tuned at various values in the vicinity of the optimum tuning for the first bending mode. The variable tuning was achieved by using the tuning electronics described previously. The purpose of the test was to determine the sensitivity of the truss first mode damping level to variations in the RSP's tuning parameters away from optimum. This information is important since optimum tuning can rarely be accomplished from the model alone, and deviations from optimum values can result in great losses in damper performance.

Two variation tests were conducted. The first involved setting the inductor to obtain the optimum δ or inductor value and then varying the resonant circuit resistance. The second test entailed setting the damper to the optimum value of the electrical circuit resistance and varying the inductor value from below to above optimum, thus varying the frequency tuning ratio. The results from these experiments are thus comparable to the results for the parameter variation of the PMD.

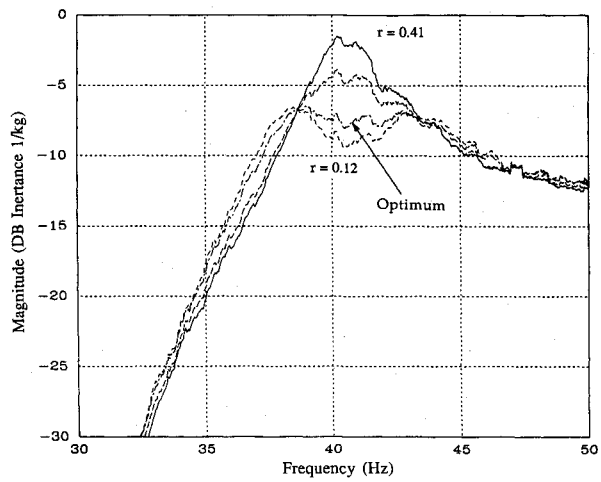

Fig. 8a First mode RSP dissipation parameter variation from $r = 0.12$ (widely spaced modes) to $r = 0.41$ (single mode).

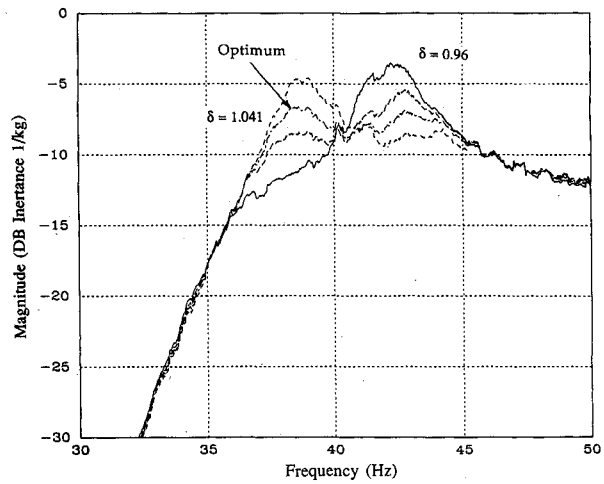

Fig. 8b First mode RSP frequency tuning parameter variation from $\delta = 0.96$ (single mode above 40 Hz) to $\delta = 1.041$ (single mode below 40 Hz).

The system transfer functions that resulted from the first variation of the RSP damper resistance can be seen in Fig. 8a. The resonant piezoelectric exhibits the same mode coalescence present in the PMD variation. Increasing damping from below optimum to above results in the convergence of two relatively undamped modes into a single damped mode and finally into a single undamped mode. This behavior is common in the PMD resonant damper as well.

The transfer functions that result from the frequency tuning variation at optimal shunting resistance are shown in Fig. 8b. As the damper frequency is changed from below to above optimal, the system mode drops on the right and then rises on the left. Thus, although the tuning requirements for the RSP are different from the PMD, the RSP shares some fundamental properties with it. Among these are the sensitivities to parameter variations and dependence on a single parameter for determination of the damper performance. For PMDs, this is the mass ratio β; for piezoelectrics, it is the generalized electromechanical coupling coefficient K_{31}^2.

IV. Summary and Conclusions

A complete testing plan has been executed with the purpose of investigating damping enhancement schemes on a realistic 10-bay truss structure. Two resonant damping schemes were implemented on the experimental truss. The first scheme utilized a space-realizable linear electromechanical actuator to form a proof-mass damper (PMD); the second utilized the piezoelectric truss members in a resonant shunted piezoelectric (RSP) damping application.

The designs of the main experimental components were reviewed. These components were the experimental truss test article, the damping mechanisms, and their supporting electronics. The experimental test article was designed to provide a low damping base structure upon which the damping enhancement could be tested. A truss was chosen as the experimental article because a complex structure was required to ascertain the practicalities of the damping enhancement implementations.

The PMD consisted of a linear dc motor, with the magnetic circuit part of the motor serving as the proof mass. The actuator was made tunable by the addition of negative position and velocity feedback to produce electrical springs and dampers for the system.

The RSP was implemented with piezoelectric truss members consisting of cylindrical piezoceramics and a fibrous composite outer shell. These members replaced the standard aluminum members in the truss. The electrodes of these members could be wired together and shunted by resonant electrical circuitry to maximize energy dissipation. A variable circuit allowed the resonant piezoelectric damper to be tuned optimally to the structural modes.

Experiments were performed to measure the effectiveness of two types of dynamic passive damping mechanisms, the classical PMD and a new technique involving piezoelectric materials shunted with resonant electrical circuits (RSP). The PMD implementation was shown to be able to achieve 6.4% of critical damping in the first mode with a mass ratio of 2.7% (not including tuning circuitry and amplifiers). The RSP implementation raised the first mode system damping to 6.0% with a mass penalty of only 1.9% of the total system mass (piezoelectric members and inductor). The RSPs are thus competitive with PMDs in mass efficiency and much simpler mechanically.

This mechanical simplicity makes the RSP damping methodology better suited to low-amplitude applications than the current PMD design. The friction effects in the current PMD design would dominate in low-amplitude applications, and a different support system, perhaps using flexures, would be required to eliminate these effects.

The experiments conducted with mistuned resonant dampers indicated that the obtainable damping enhancement decreased sharply with deviation from the optimal tuning parameters. This sensitivity made it difficult to tune the resonant dampers optimally using only a model for guidance. The system trends associated with a given mistuning were found to be the same for both the PMD and the RSP.

Mechanical PMD and electrical RSP dynamic vibration absorber concepts have been shown to be practical, effective methods for augmenting the natural damping of trusswork structures. Although applicable only to narrow-band damping applications, the resonant dampers were able to achieve modal damping ratios from 6 to 7% with only 2 to 3% increase in total system mass. The RSP damping methodology in particular was shown to be a more mechanically simple and mass-efficient alternative to the proof-mass damper for truss damping applications.

Acknowledgments

This work was sponsored by NASA Grant NAGW-21 with Samuel Venneri serving as technical monitor. The authors also wish to thank Andreas von Flotow and Walter Chung for their contributions to this work.

References

[1]Ashley, H., and Edberg, D. L., "On the Virtues and Prospects for Passive Damping in Large Space Structures," *Proceedings of the Damping '86 Conference,* Flight Dynamics Lab., Air Force Wright Aeronautical Labs., OH, Rept. AFWAL-TR-86-3059, March 1986, pp. DA-1–DA-7.

[2]Skelton, R. E., "Algorithm Development for the Control Design of Flexible Structures," *Proceedings of the Modelling, Analysis, and Optimization Issues for Large Space Structures,* NASA CP-2258, May 1982.

[3]Hagood, N. W., and Crawley, E. F., "Development and Experimental Verification of a Damping Enhancement Methodology for Space Structures," Space Systems Lab., Dept. of Aeronautics and Astronautics, Massachusetts Inst. of Technology, Cambridge, MA, Rept. 18-88, 1988.

[4]Chen, G., and Wada, B. K., "Passive Damping for Space Truss Structures," *Proceedings of the 29th AIAA/ASME/ASCE/AHS Structures, Structural Dynamics, and Materials Conference,* AIAA, AIAA Paper 88-2469, Washington, DC, May 1988, pp. 1742–1749.

[5]Miller, D. W., and Crawley, E. F., "Theoretical and Experimental Investigation of Space-Realizable Inertial Actuation for Passive and Active Structural Control," *Journal of Guidance, Control, and Dynamics,* Vol. 11, No. 5, 1988, pp. 449–458.

[6]Juang, J., "Optimal Design of a Passive Vibration Absorber for a Truss Beam," *Journal of Guidance, Control, and Dynamics,* Vol. 7, No. 6, 1984, pp. 733–739.

[7]Fanson, J., Blackwood, G., and Chu, C., "Active-Member Control of Precision Structures,"*Proceedings of the 30th AIAA/ASME/ASCE/AHS Structures, Structural Dynamics, and Materials Conference,* AIAA, AIAA Paper 89-1329, Washington, DC, May 1989, pp. 1480–1494.

[8]Peterson, L., Allen, J., Lauffer, J., Miller, A., and Skelton, R., "An Experimental and Analytical Synthesis of Controlled Structure Design," *Proceedings of the 30th AIAA/ASME/ASCE/AHS Structures, Structural Dynamics, and Materials Conference,* AIAA, AIAA Paper 89-1170, Washington, DC, May 1989, pp. 91–103.

[9]Hagood, N. W., and Crawley, E. F., "Approximate Frequency Domain Analysis of Linear Damped Space Structures," *AIAA Journal,* Vol. 28, No. 1, 1990, pp. 1953–1961.

[10]"Components Catalogue Construction M12," MERO-Raumstruktur GmbH & Co., Wuerzburg, Germany, 1985.

[11]Timoshenko, S., Young, D. H., and Weaver, W., Jr., *Vibration Problems in Engineering,* 4th ed., Wiley, New York, 1974, pp. 273–278.

[12]Zimmerman, D. C., Inman, D. J., and Horner, G. C., "Dynamic Characterization and Microprocessor Control of the NASA/UVA Proof Mass Actuator," *Proceedings of the 25th AIAA/ASME/ASCE/AHS Structures, Structural Dynamics, and Materials Conference,* AIAA, New York, May 1984, pp. 573–577.

[13]Hagood, N. W., and von Flotow, A., "Damping of Structural Vibrations with Piezoelectric Materials and Passive Electrical Networks," *Journal of Sound and Vibration,* Vol. 146, No. 2, 1991, pp. 243–268.

[14]"Data for Designers," Vernitron Piezoelectric Div., Bedford, OH.
[15]Crawley, E. F., and de Luis, J., "Use of Piezoelectric Actuators as Elements of Intelligent Structures," *AIAA Journal,* Vol. 25, No. 10, 1987, pp. 1373–1385.
[16]Fanson, J. L., and Caughey, T. K., "Positive Position Feedback Control for Large Space Structures," *Proceedings of the 28th AIAA/ASME/ASCE/AHS Structures, Structural Dynamics, and Materials Conference,* AIAA, Washington, DC, April 1987, pp. 588–598.
[17]Hanagud, S., Obal, M. W., and Calise, A. J., "Optimal Vibration Control by the Use of Piezoceramic Sensors and Actuators," *Proccedings of the 28th AIAA/ASME/ASCE/AHS Structures, Structural Dynamics, and Materials Conference,* AIAA, Washington, DC, April 1987, pp. 987–997.
[18]Bailey, T., and Hubbard, J. E., "Distributed Piezoelectric Polymer Active Vibration Control of a Cantilever Beam," *Journal of Guidance, Control, and Dynamics,* Vol. 8, No. 5, 1985, pp. 605–611.
[19]Lee, D. T., Morf, M., and Friedlander, B., "Recursive Least Squares Ladder Estimation Algorithms" *IEEE Transactions on Acoustics, Speech, and Signal Processing,* Vol. ASSP-29, No. 3, 1981, pp. 627–641.